Pacific Northwest National Laboratory
Operated by Battelle for the
U.S. Department of Energy

Foaming of E-Glass (Report for G Plus Project for PPG)

D. Kim   P.. Hrma
Pacific Northwest National Laboratory

B. Dutton   L. Pilon
University of California, Los Angeles

April 2004

DISCLAIMER

Foaming of E-Glass (Report for G Plus Project for PPG)

Dong-Sang Kim
Pavel R. Hrma
Pacific Northwest National Laboratory

Bryan C. Dutton
Laurent Pilon
University of California, Los Angeles

April 2004

Pacific Northwest National Laboratory
Richland, Washington 99352

Abstract

The behavior of foams generated in the crucible melts was investigated to study the effect of furnace atmosphere on E-glass foaming, specifically focused on its water content to understand the effect of oxy-firing. A quartz-crucible furnace equipped with video recording was used to observe the behavior and to evaluate stability of foams generated from the PPG E-glass under various atmospheres. The present study preliminarily concluded that the higher foaming in oxy-fired furnace compared to air-fired is caused by the effect of water on early sulfate decomposition, promoting more efficient refining gas generation from sulfate (known as "dilution effect"), not by the effect of humidity on foam lamella stability. A plausible explanation for the difference between soda-lime glass and E-glass in the end result of the dilution effect on glass refining and foaming is presented. A preliminary experiment on the effect of heating rate also suggests that thermal history of glass melting can be a major factor in the rate of E-glass foaming. Approaches to develop the methods to reduce foaming in oxy-fired furnace are recommended.

Contents

Figures

Tables

1.0   Introduction

Glass foams generated in glass-melting furnaces reduce energy efficiency and can lead to poor glass quality. Foaming of E-glass refined with sulfate is especially severe when processed with oxy-fuel firing. The objective of this project was to study the effects of the furnace atmosphere, mainly its water content, on E-glass foaming. The ultimate goal is to identify conditions for foam reduction during E-glass processing.

Most of the studies of foaming in silicate melts focused on soda-silicate or soda-lime-silicate melts (Kim and Hrma 1991 and 1992; Hrma and Kim 1994; Laimböck 1998), or on metallurgical slags (Cooper and Kitchener 1959; Zhang and Fruehan 1995). Pilon et al. (2001) provides through reviews of the literature; they also collected data on foaming and correlated the extent of foaming of different high-viscosity liquids with their properties. Unfortunately, little data exist on foaming in E-glass.

Cable *et al*. (1968), who studied the foaming of binary silicate melts, observed that foaming temperature was lower and foam volume was higher in wet atmospheres; also, foam was more stable in pure oxygen, whereas glass did not foam in a pure nitrogen atmosphere. Kappel *et al*. (1987) observed that increasing the partial pressure of SO_2 destabilized foam. It has also been observed that foaming increases with the pull rate, the use of recycled and contaminated cullet of mixed colors (Laimböck 1998). The type of gaseous fuel used to heat the melt and also the luminosity of the flame it produces were reported to affect the foam of iron slags (Cooper and Kitchener, 1959).

It is generally believed that severe foaming in oxy-fuel-fired furnaces is caused by a higher partial pressure of water in the furnace atmosphere (Laimböck, 1998). However, even for soda-lime glasses and metallurgical slags, the effect of water on foaming is not clearly understood and reported experimental data appear to be contradictory. For example, Cable *et al*. (1968) and Laimböck, 1998 reported that wet atmosphere increased foaming, whereas Kappel *et al*. (1987) showed that humidity in the atmosphere destabilized the foam. Water reduces viscosity, thus reducing foam stability by enhancing foam drainage. Water also reduces surface tension (Parikh, 1958).[1] However, the effect of surface tension on foam stability depends more on its change with time or its gradient across the foam film thickness.

Laimböck (1998) studied the effect of water content in air atmospheres on the foaming of soda-lime glass batch and found that the foam formation started at a lower temperature and the maximum foam volume (and total foam volume) increased as the water content in air increased from 0 to 55%. Laimböck measured the sulfate content in glass before and after foaming and found that the sulfate loss during foaming increased as the water content increased. This increased sulfate loss (lower sulfate retention) at higher water content was responsible for higher foaming. As dissolved water content in glass increases, the partial pressure of H_2O in bubbles also increases, thus diluting the fining gas concentration in bubbles and promoting the transfer of fining gases from the melt into bubbles. In other words, water vapor in

---

[1] According to Parikh (1958), polar gases such as sulfur dioxide (SO_2), ammonia (NH_3), hydrogen chloride (HCl), and water vapor (H_2O) lower the surface tension, whereas nonpolar gases such as dry air, dry nitrogen, helium and hydrogen have no effect. Among the polar gases cited, water has the largest dipole moment and therefore has the strongest effect on the surface tension. Parikh (1958) showed that the surface tension decreases with the square root of the partial pressure of water.

bubbles decreases the partial pressure of fining gases, thus increasing the driving force for their transfer from melt and shifting the equilibrium towards a more extensive decomposition of the fining agents. As a result, sulfate begins to decompose at a lower temperature and its decomposition continues to a lower sulfate level retained. This mechanism was mathematically formulated as the "dilution model" (Laimböck, 1998). Water in the atmosphere helps the refining action of the sulfate, making it possible to lower the addition of sulfate to obtain an equal refining efficiency compared to dry atmosphere.

Numerous laboratory studies (Cable *et al*. 1968; Kappel *et al*. 1987; Kim and Hrma 1991 and 1992; Hrma and Kim 1994; Laimböck 1998) used one of the two methods for foam generation in molten glass:
1. Refining gases are generated by increasing temperature or reducing pressure; this creates transient foam that grows and collapses
2. Gas is bubbled into a glass melt at a constant temperature; this produces a foam of a constant height

The initial effort in this project focused on establishing the methodology for generating transient and steady-state foams in a reproducible manner. A quartz-crucible furnace equipped with video recording was used to observe the behavior and to evaluate the stability of foams generated from the PPG E-glass under various atmospheres, including CO_2, O_2, N_2 and H_2O.

2.0   Preliminary Studies

This section describes preliminary studies to establish foam generation methodology and identify factors that affect foam stability.

2.1   Experimental Set-up

A box furnace with a silica-glass window at the front door was used in foaming experiments (Figure 1). A sample of glass batch or melt was placed in a silica-glass cylindrical crucible of 2-cm inner diameter. The sample height-to-width ratio was recorded by a video camera with a long-focus lens. The sample height was determined from the known diameter of the cylindrical crucible. The furnace had a rear recess that was kept at a lower temperature than the crucible area to provide a darker background for a better contrast at high temperatures.
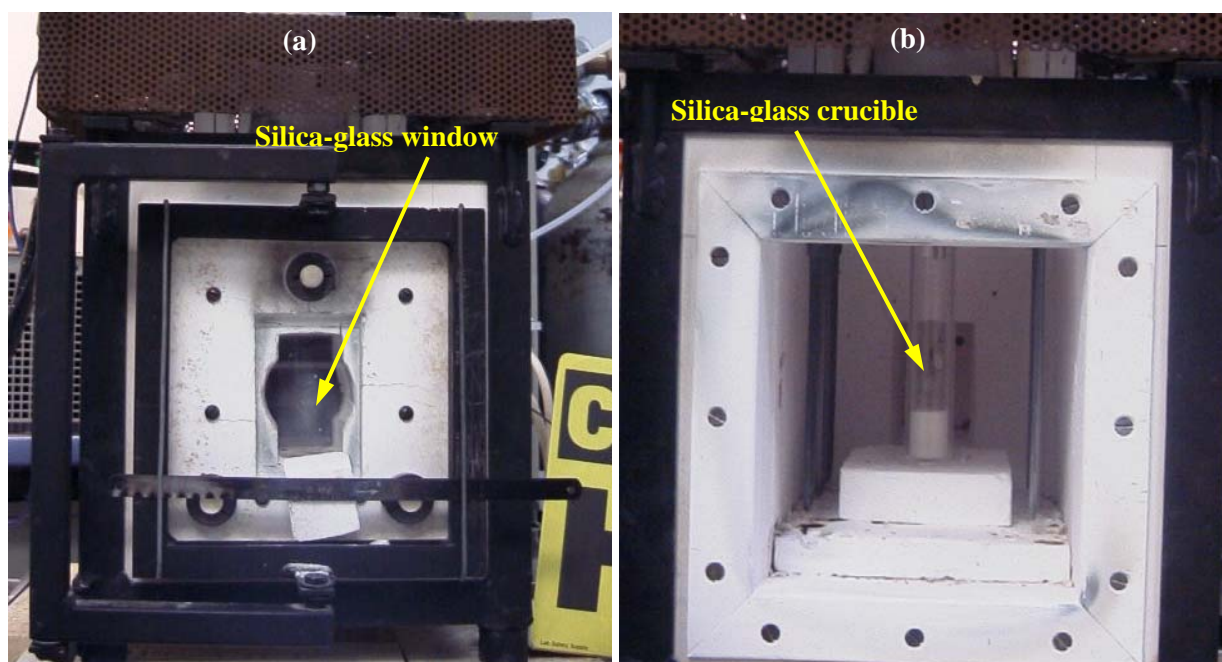
Figure 1. The door (a) and the interior (b) of the test furnace with a silica-glass crucible

2.2   E-glass Batches

The E-glass batch received from PPG contained all the raw materials in prescribed proportions except for sodium sulfate. In the present study, batches were mixed with 0.14 mass% sodium sulfate (corresponding to 0.17 mass% SO_3 in glass including the sulfate introduced as impurity from other raw materials).

2.3   Transient Foam

The purpose of the preliminary transient foam studies was twofold:

- to determine the pre-melting temperature of the batch
- to determine conditions for foam experiments in the present set-up.

The initial two transient foam experiments were conducted with PPG E-glass batch containing 0.14 mass% sodium sulfate. The batch was loaded in a cylindrical crucible of 2-cm inner diameter and 10-cm height. The first experiment was performed with a 5-g batch heated at 10 °C/min from 300 to 1500°C and kept at 1500°C. Figure 2 shows sample height and furnace temperature versus time. The batch began to shrink and melt at about 1140°C. The melt height began to increase due to foaming at about 1370°C. The foam eventually rose beyond the observable range of the present set-up, so the maximum foam height could not be recorded.

The second experiment was conducted with 4-g batch at 5 °C/min heating rate—see Figure 3. The collapse side of the foam-height curve (marked by the dotted line) is subjected to some uncertainty because the visibility of the foam level was decreased by the glass melt attached to the crucible wall. Figure 4 compares the height of the samples per mass unit of batch, i.e., h/m_B, where h is the foam height and m_B is the mass of the batch. If the gas phase is uniformly distributed throughout the glass phase, then the foam volume per batch mass, $v_{FB} = Ah/m_B$, where A is the cross-section area of the cylindrical crucible. Figure 4 shows that the maximum foam height is lower when the rate of heating is slower.

This observation can be rationalized as follows. Let us suppose for simplicity that gas phase from decomposing sulfate is all stored in the melt until the melt reaches a certain high temperature T_2; say $T_2 = $ 1470°C, at which the gas phase is rapidly released. Let us further assume that the sulfate begins to decompose at a certain temperature T_1; say $T_1 = 1370$°C. Let v_G be the volume of gas generated in the melt and R_a the average rate of gas release from the foam within the temperature interval from 1370°C to 1470°C and $\Phi = \mathrm{d}T/\mathrm{d}t$ the rate of temperature increase (T is the temperature and t is time). Then the volume of gas retained in the foam when temperature is raised from 1370°C to 1470°C is $v_F = v_G - R_a(t_2 - t_1)$, where t_2 is the time at which the sample temperature was T_2 and t_1 the time at which the sample temperature was T_1. If the heating rate was constant, then $v_F = v_G - r_a(T_2 - T_1)/\Phi$. It follows that the volume of gas retained within the melt foam is proportional to the rate of heating.

As Figure 4 shows, the initial batch height per batch mass, which is proportional to the batch specific volume, considerably varies from experiment to experiment. This result is caused by a difference in packing density of batch particles in each experiment, which was not a variable deliberately controlled. However, as expected, the melt height before foaming is similar in both experiments; the differences are caused by the different content of the residual gas in the samples. The final height per batch mass of the refined melt was the same from experiment to experiment.
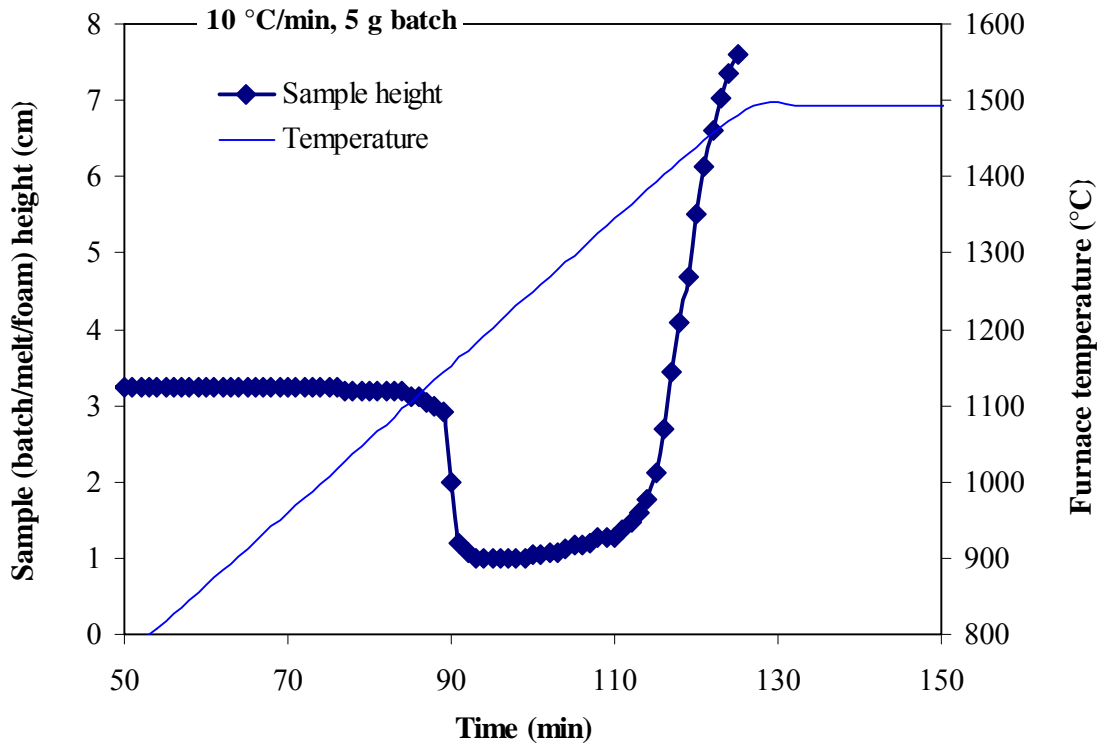
Figure 2. Sample Height versus Time in the E-Glass Batch Ramp-Heated at 10 °C/min
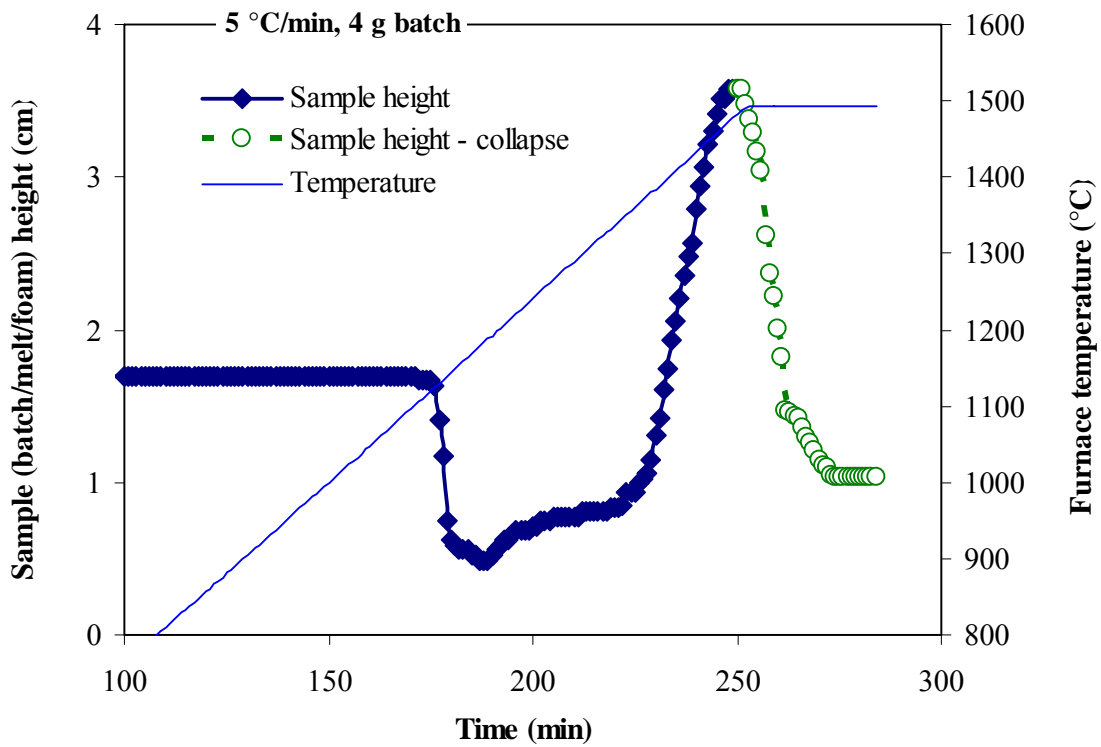
Figure 3. Sample Height versus Time in the E-Glass Batch Ramp-Heated at 5 °C/min
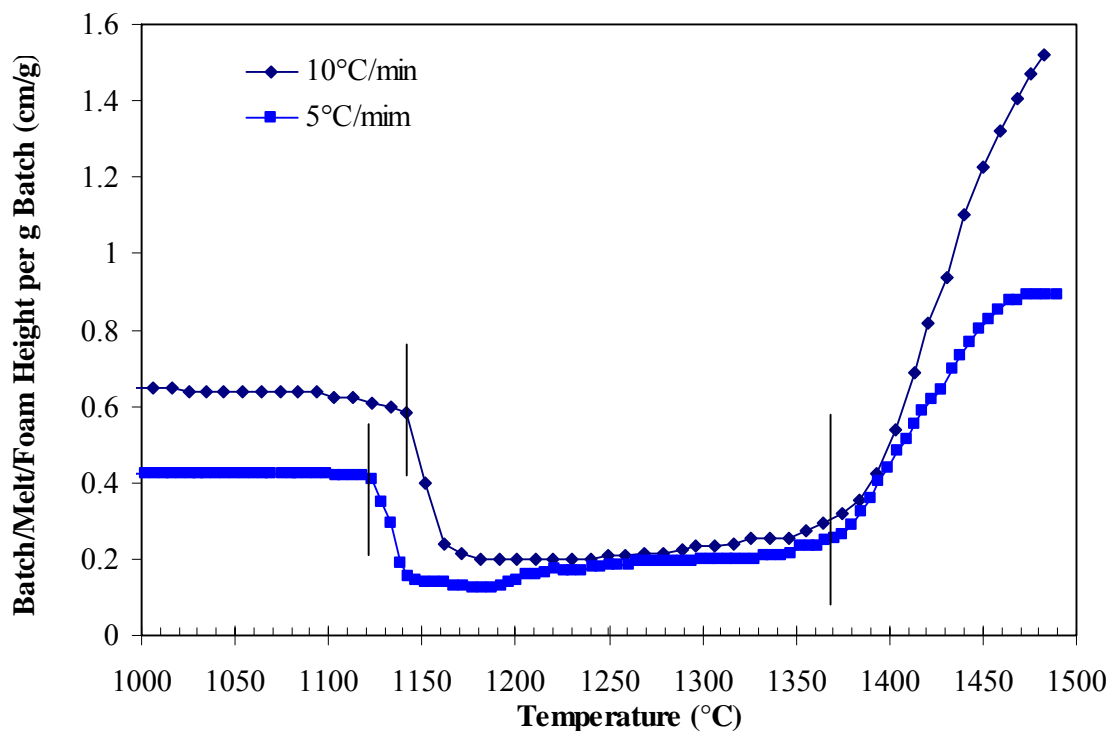
Figure 4. Sample Height per Unit Mass of Batch versus Temperature

2.4 Pre-melting Trial

We also realized that pre-melting the batch at a temperature below 1380°C would minimize compositional variability and would considerably reduce the time required to complete an experiment. The pre-melting should be done at a temperature high enough to obtain homogeneous melt but low enough to retain most of the sulfate.

To make pre-melted glass, the glass batch with 0.14 wt% sodium sulfate was melted at 1380°C for 2 h and ground into powder. When this glass was remelted at 1380°C and held for 30 min at this temperature, a ramp heating to 1500°C at 5 °C/min did not produce any foam. We reasoned that a large fraction of sulfate probably decomposed, leaving not enough sulfate to generate foam, during melting at 1380°C. Also, the destruction of nucleation sites for bubbles during pre-melting could hinder foaming. Therefore, we gave up pre-melting and continued foaming experiments with the glass batch.

Based on these scoping tests, we determined the following condition for transient foam experiments:
- Conduct foaming experiments with glass batch
- Use the initial batch mass of 4 g
- Heat samples at the rate of 5 °C/min

These conditions produced an adequate maximum foam height for our experimental setup and 5 °C/min is believed to be close to the typical heating rate of the batch in the glass furnace (Hrma 1982).

2.5 Steady State Foam

Steady-state foam is produced by bubbling gas into the melt. Therefore, it allows the gas compositions to be controlled. For example, the effect of a sudden change of gas composition in bubbles and the difference in gas composition in bubbles and the surrounding atmosphere on foam behavior can be investigated. The complications of the kinetics of glass producing reactions that are inevitable in transient foam studies do not occur when foam is produced by bubbling gas from the external source. On the other hand, steady state experiments do not simulate the fining process of the glass as produced in the real furnace. Therefore, they can elucidate certain important aspects of foam behavior, but necessitate separate studies of the reaction kinetics of foaming agents.

To produce a steady-state foam, PPG E-glass cullet was broken into pieces and melted in a cylindrical quartz crucible (ID = 2.0 cm) by rapidly heating to 1450°C. A platinum tube (ID = 3 mm) was lowered into the molten glass so that its tip was submerged approximately 1.5 cm below the melt surface. Compressed air, regulated by a flow meter, was injected into the melt through the tube. The melt was monitored by the video equipment.

The injected bubbles were bursting at the melt surface without creating foam. The melt from ruptured bubbles obscured crucible walls, making observations increasingly difficult as the test progressed. It seemed that bubbles were large compared to the crucible diameter and the depth of the tube orifice. A rough estimate of the bubble size, using the formula $R_B = (3R_O\sigma/2\rho g)^{1/3}$, where R_O is the tube outer diameter, σ is the melt surface tension, ρ is the melt density, and g is the acceleration due to gravity, yields $2R_B = 7$ mm. The viscosity affects the velocity at which the bubble ascends to the surface and hence the distance that separates two consecutive bubbles. To obtain right conditions for generating steady-state foam would require varying crucible diameter, bubbling depth, tip diameter, and melt temperature. However, further attempts to produce foam by bubbling through the melt were discontinued within this study.

.

3.0   Transient Foam Studies

3.1   Experimental Procedures

A 4-g of E-glass batch with 0.14 mass% Na_2SO_4 was placed in a cylindrical silica-glass crucible of 2.0-cm inner diameter and 30-cm high and ramp-heated in the furnace shown in Figure 1 from 300°C to 1500°C at 5 °C/min. Figure 5 shows a schematic of the experimental set-up used to control the atmosphere above the sample surface. The batch was initially heated under ambient atmosphere and gas, such as air or carbon dioxide, was introduced into the crucible when the temperature reached 1250°C. Humidity was controlled by bubbling compressed gas through water held in a flask at a constant temperature. The tube conducting gas from the flask to the crucible was heated via insulated resistive heating coil wrapped around the gas tube to prevent condensation of water in the gas inlet system. The tip of the gas inlet tube was placed well above the melt surface to minimize its effect on the temperature inside the crucible. For the same reason, the heating coil was turned on in all tests regardless of humidity in the gas mix.
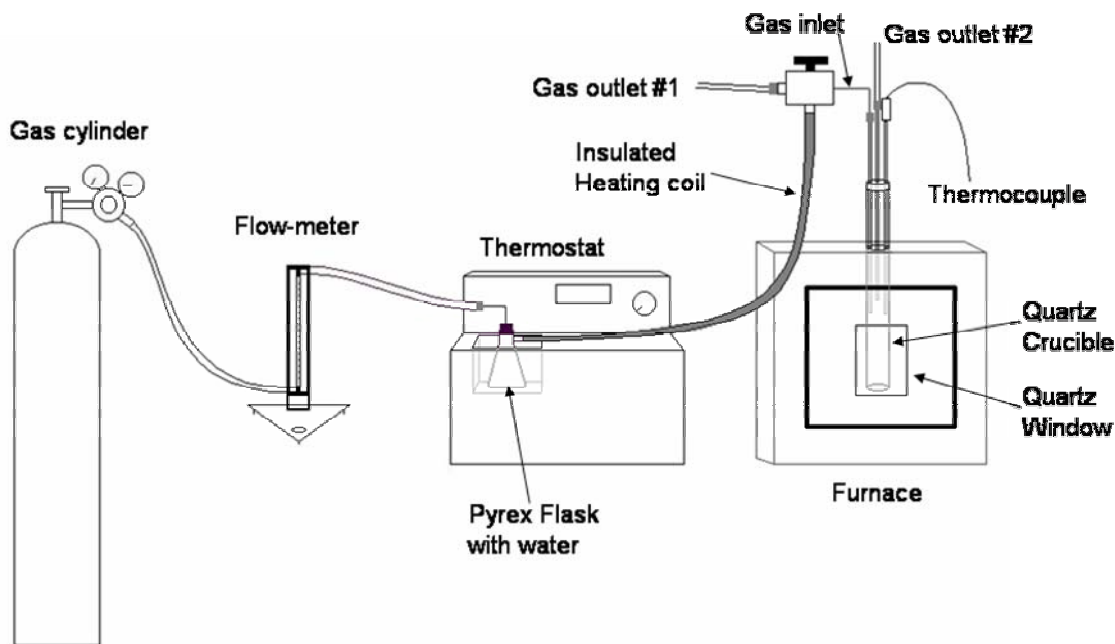
Figure 5. Schematic of Experimental Set-up for Transient Foam Study Using Controlled Atmosphere

The flow of the gas was set at 40 cm^3/min for most tests. This rate was deemed sufficiently low to avoid mechanical agitation of the foam and a decrease of the temperature above the melt while maintaining a constant atmosphere. At this flow rate, the gas content in the crucible would be renewed roughly every 2 min. The flow rate of gas was measured before the gases are humidified; thus, the actual flow rate was higher for atmospheres containing H_2O.

Table 1 summarizes the test conditions used in the present study. It is assumed that dry air was composed of 80% N_2 and 20% O_2 and the gases introduced in the flask reached equilibrium H_2O concentration. Although the amount of H_2O in each condition was not measured, it is assumed that the actual water content does not significantly deviate from the calculated value given the slow gas flow rate.

Table 1. Description of Tests and Calculated Gas Compositions

Test #	Description	Gas Volume%			
		N_2	O_2	CO_2	H_2O
1	Air	80	20		
2	Air, repeat of #1	80	20		
3	Air, higher flow rate[(a)]	80	20		
4	Air + 20% H_2O	64	16		20
5	Air + 55% H_2O	36	9		55
6	CO_2			100	
7	CO_2 + 20% H_2O			80	20
8	CO_2 + 55% H_2O			45	55
9	(CO_2 + 55% H_2O) + 10% O_2		10	40.5	49.5
10	CO_2 + 20% O_2		20	80	
11	CO_2 + 20% N_2	20		80	
12	CO_2 + 80% N_2	80		20	
13	CO_2 + 55% H_2O[(b)]			45	55

[(a)] The flow rate of 90 cm^3/min instead of 40 cm^3/min used for all other tests.
[(b)] Gas was introduced from 300°C instead of 1250°C used for all other tests.
The Test # does not represent the actual order of tests performed.

3.2 Results

The following results are shown in the form of gas phase-to-liquid phase volume ratio, ψ, defined as

$$\psi = \frac{V_g}{V_m} \tag{1}$$

where V_g is the volume of gas in the sample and V_m is the volume of melt in the sample. Obviously, $V_g = V - V_m$, where V is the sample volume. Hence, by Equation (1),

$$\psi = \frac{V}{V_m} - 1 \tag{2}$$

If the sample shape is a vertical cylindrical column of a constant cross-section area, $V/V_m = H/H_m$, where H is the sample height and H_m is the height of a gas phase-free sample. While H is measured from the video record, H_m cannot be obtained in the same way because the initial sample is batch and when the batch melts, the sample contains bubbles until all foam collapses, but then some melt remains spread on the crucible walls. Therefore, H_m must be calculated using the formula

$$H_m = \frac{m_b f_b}{A\rho_m} \qquad\qquad (3)$$

where m_b is the mass of the batch loaded into the crucible, f_b is the melt-to-batch mass ratio, A is the crucible inner cross-section area, and ρ_m is the melt density.

For the PPG glass, $f_b = 0.899$, $\rho_m = 2.45$ g/mL (at 1350°C), $A = \pi r_c^2$, where $r_c = 10$ mm is the crucible inner radius, and $m_b = 4.00$ g for all experiments. Hence,

$$H_m = 4.67 \text{ mm} \qquad\qquad (4)$$

To avoid the time shift between experiments, the time was set to zero when the furnace temperature reached 1300°C. Figure 6 displays ψ and T as functions of time. The target temperature history (ramping at 5 °C/min to 1500°C) is also shown.

Typically, ψ reaches maximum at a temperature below 1500°C. As Figure 6 shows, the actual temperature history somewhat differs from the targeted one (the rate of heating slows down before reaching the final temperature) and the final temperature slightly differs from experiment to experiment, but the time-temperature curves up to the final temperature are almost identical. The inability to keep the final temperature the same in each experiment is inherent in the current experimental setup. Consequently, the foam starting temperature, maximum foam height, and foam generation rate occurred under well-controlled experimental conditions, whereas the foam collapse occurred at temperatures that were not exactly identical, not to mention the poor visibility of the collapsing sample caused by bursting of bubbles that obscured the crucible wall.

For the three tests with air flow, for which ψ versus t is displayed in Figure 6, the average maximum ψ was $\psi_{max} = 7.00$ with a standard deviation of 0.46, corresponding to the reproducibility conservatively estimated at 13%. Figure 7 contains ψ versus t plots for all tests performed to show overall range of the foam behavior. Figure 8 through Figure 10 show ψ versus t plots for experiments conducted under different atmospheres: dry and humid air in Figure 8, dry and humid CO_2 in Figure 9, and various dry atmospheres in Figure 10. Figure 7, Figure 8, and Figure 10 include ψ versus t for the Test #1 (air) only from the three tests with air flow. Table 2 summarizes ψ_{max} data.
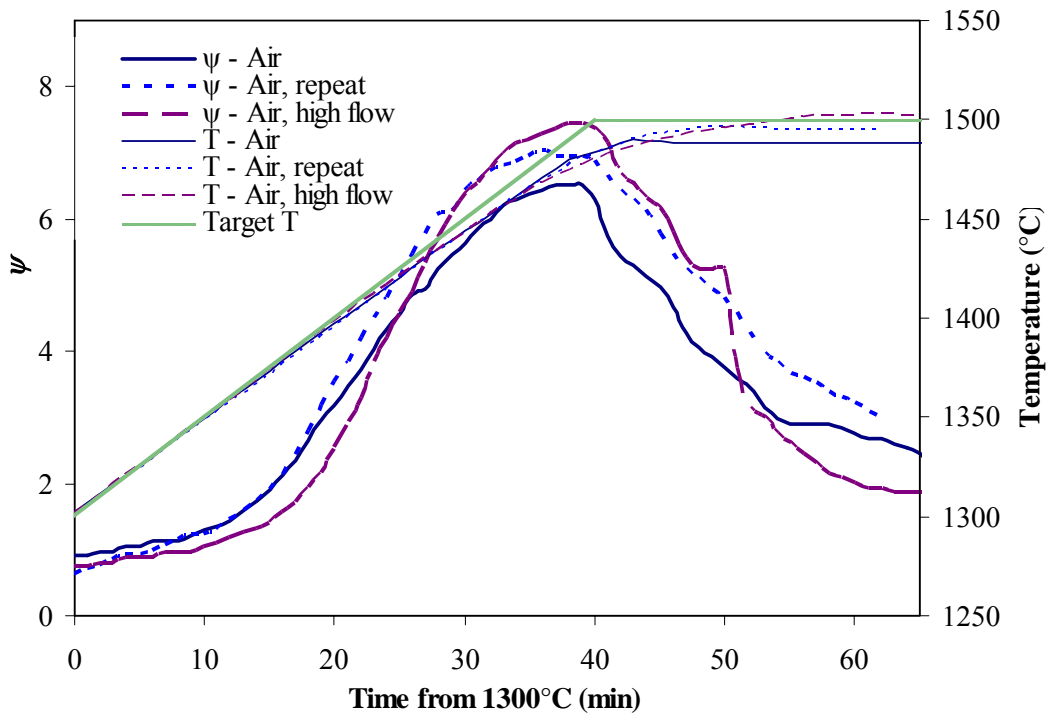
**Figure 6.** ψ and Furnace Temperature versus Time (= 0 at T = 1300°C) for the Tests with Air Flow
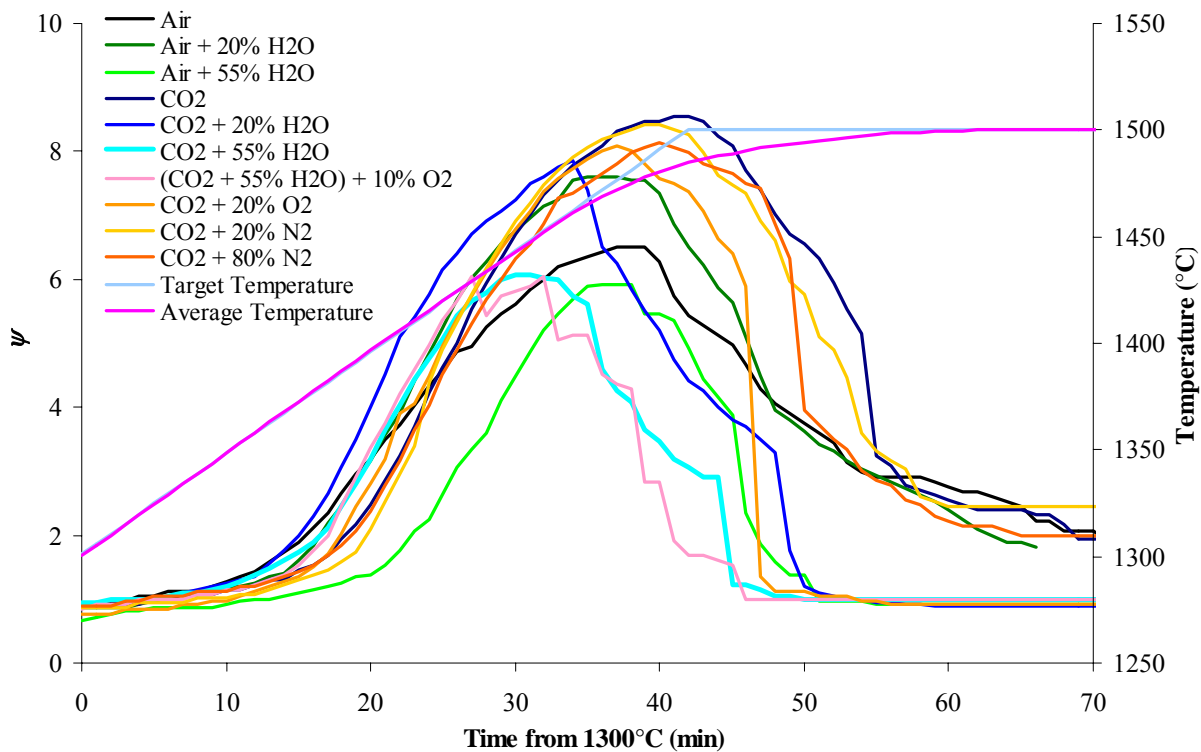

Figure 7. ψ and Furnace Temperature versus Time for All Tests
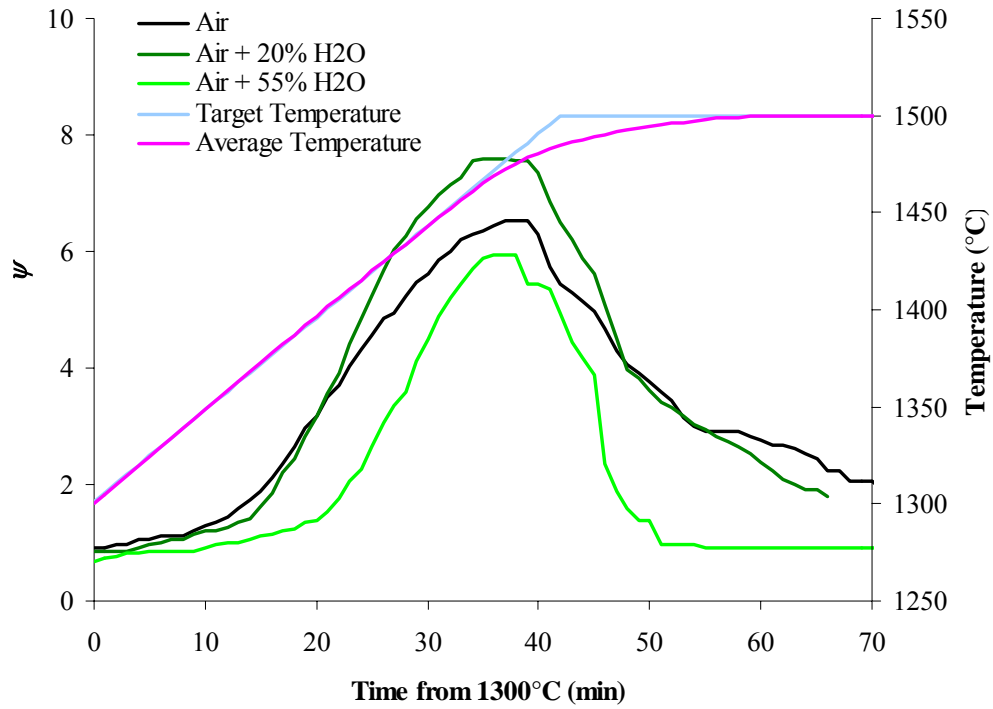
Figure 8. ψ and Furnace Temperature versus Time for Tests in Air-Based Atmospheres
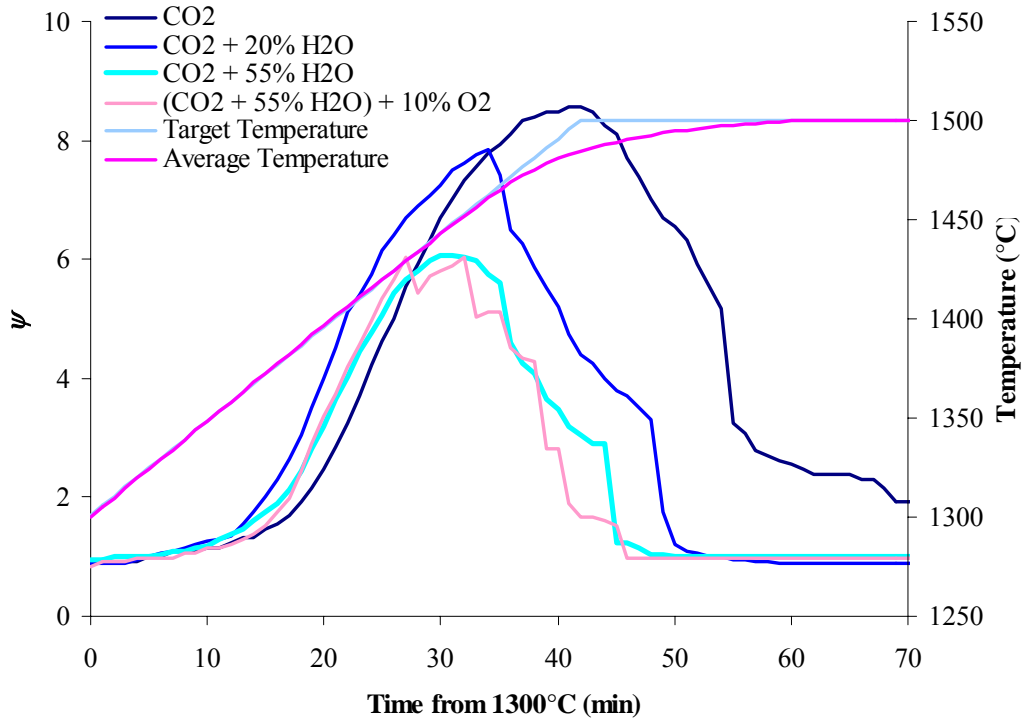
Figure 9. ψ and Furnace Temperature versus Time for Tests in CO_2-Based Atmospheres
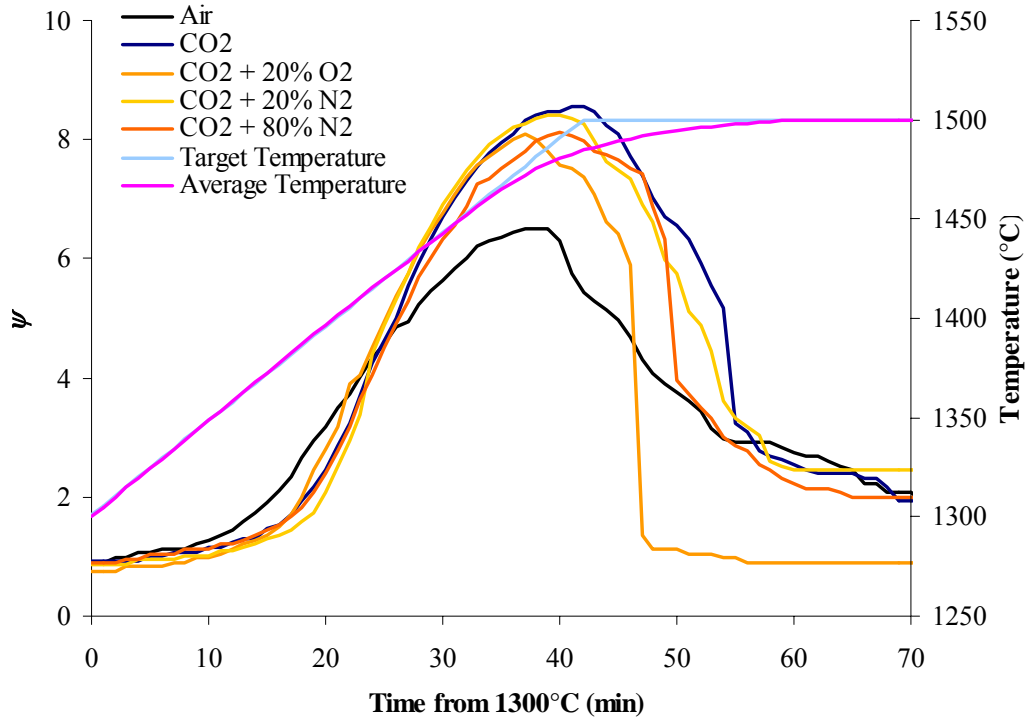
Figure 10. ψ and Furnace Temperature versus Time for Tests in Dry Atmospheres

Table 2. Maximum ψ, ψ Increase Rates, and Foam Collapse Times for All Foaming Tests

Test #	Description	H_2O %	Max ψ	ψ increase rate		Foam collapse time (min)[a]	
				$d\psi/dt$	$d\psi/dT$	$t_{0.5}$	$T_{0.25}$
1	Air	0	6.52	0.27	0.058	16	-
2	Air, repeat of #1	0	7.03	0.33	0.070	22	-
3	Air, higher flow rate	0	7.44	0.40	0.089	14	-
4	Air + 20% H_2O	20	7.59	0.40	0.090	15	31
5	Air + 55% H_2O	55	5.93	0.37	0.079	10	13
6	CO_2	0	8.55	0.44	0.108	14	28
7	CO_2 + 20% H_2O	20	7.86	0.45	0.095	11	15
8	CO_2 + 55% H_2O	55	6.08	0.40	0.086	12	14
9	(CO_2 + 55% H_2O) + 10% O_2	49.5	6.04	0.42	0.088	12	19
10	CO_2 + 20% O_2	0	8.09	0.41	0.090	10	10
11	CO_2 + 20% N_2	0	8.41	0.42	0.087	15	-
12	CO_2 + 80% N_2	0	8.13	0.42	0.090	14	25
13	CO_2 + 55% H_2O, introduced from 300°C	Did not foam					
[a] Time to reach the specified fraction of the maximum porosity.							

13

Another way of analyzing the transient foam results is to examine the melt expansion rate, defined as $r_\psi = d\psi/dt$. There are two intervals on the foaming curve, on which r_ψ is of a nearly constant value. The first is the "primary" interval where pre-existing bubbles expand with increasing temperature. At the second interval, the bubbles grow as a result of fining reactions. The corresponding two r_ψ values were obtained from data points on these nearly linear portions of the foaming curve as illustrated in Figure 11. The low-temperature r_ψ values are virtually identical for all tests. Similarly, the $d\psi/dT$ values are obtained from the plot of ψ versus temperature. Table 2 summarizes r_ψ and $d\psi/dT$ values for the fining interval.

The foam decay is the least reproducible process under the present test conditions. It is governed by the rate of bursting of bubbles, which is a random process. In addition, the temperature at the maximum foam height slightly varied from experiment to experiment. Nevertheless, the duration of foam collapse was measured and the results shown in Table 2. The symbols $t_{0.5}$ and $t_{0.25}$ represent the times for the foam to collapse to $(1/2)\psi_{max}$ and $(1/4)\psi_{max}$, respectively (note that some samples did not reach $(1/4)\psi_{max}$ before the test was terminated).

Figure 12 and Figure 13 show the ψ_{max} and $d\psi/dT = (d\psi/dt)/(dT/dt)$, as a function of H_2O vol%; Figure 14 and Figure 15 show $t_{0.5}$ and $t_{0.25}$ as a function of H_2O vol%. Based on these plots, the major observations can be summarized as follows:

1. The foaming extent decreased as the gas humidity increased, except for 0 to 20 vol% H_2O in air. Changing air for CO_2 had little effect on foaming when humidity was 20 to 55 vol% H_2O.

2. The foaming extent was lower in dry air than in other gases tested (pure CO_2, $CO_2 + 20\% O_2$, $CO_2 + 20\% N_2$, and $CO_2 + 80\% N_2$). There was no other noticeable effect of dry gas composition on foaming.

3. The 10% O_2 addition to CO_2 with 55% H_2O had no noticeable effect on foaming.

No noticeable trend was observed in foam starting temperature between tests (1370 to 1380°C) except in air with 55% H_2O, where the foam starting temperature was noticeably higher (> 1400°C).
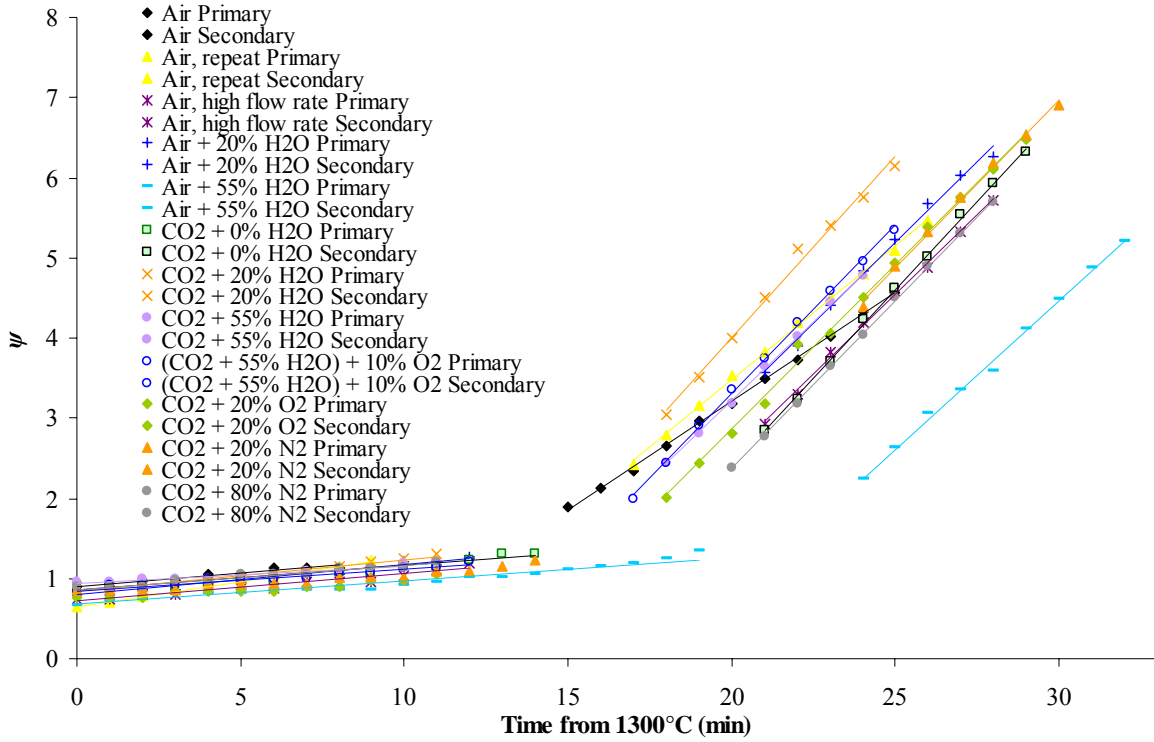
**Figure 11. ψ versus Time Showing the Selected Data Points Used for $r_\psi = d\psi/dt$**

Figure 12. Maximum ψ versus H_2O Content

15
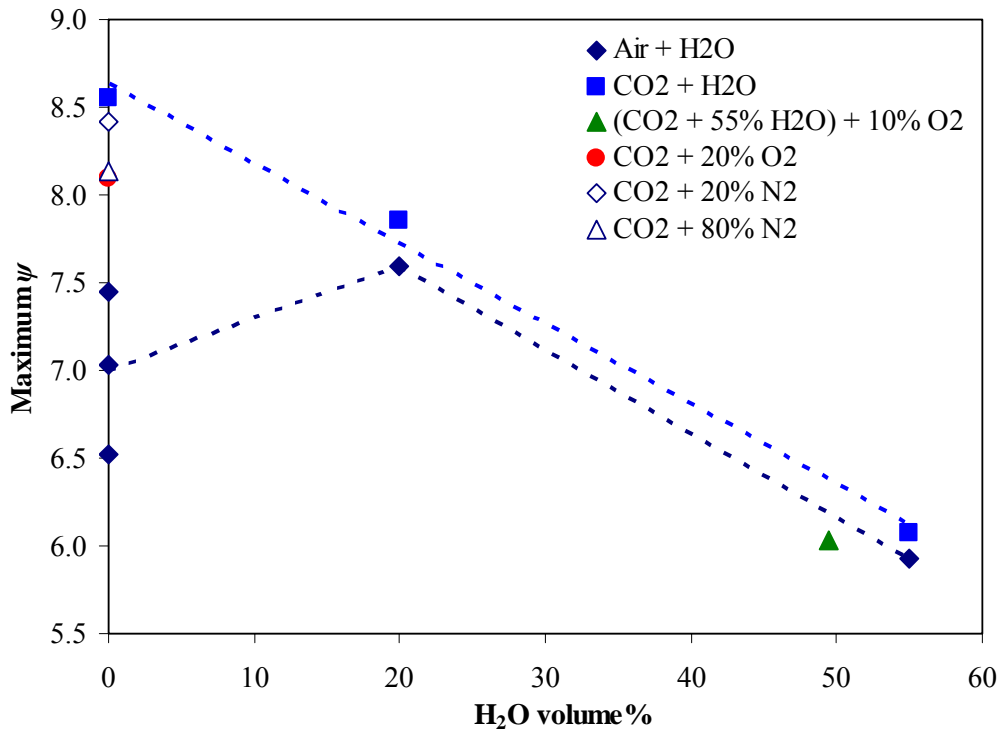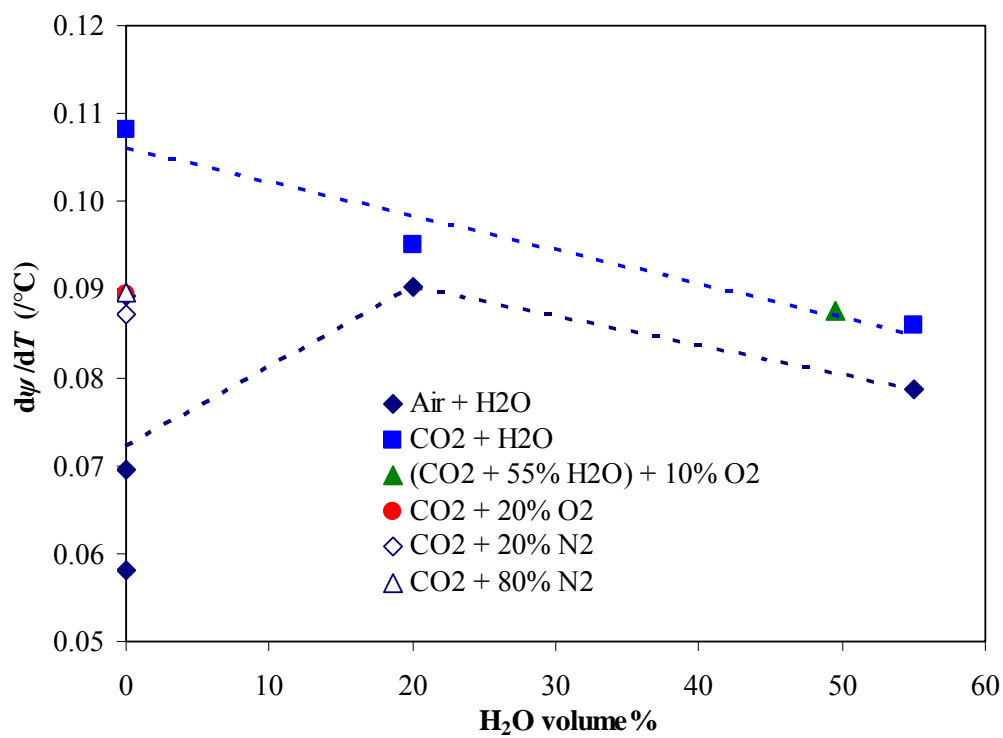
Figure 13. ψ Increase Rate (dψ/dT) versus H₂O Content
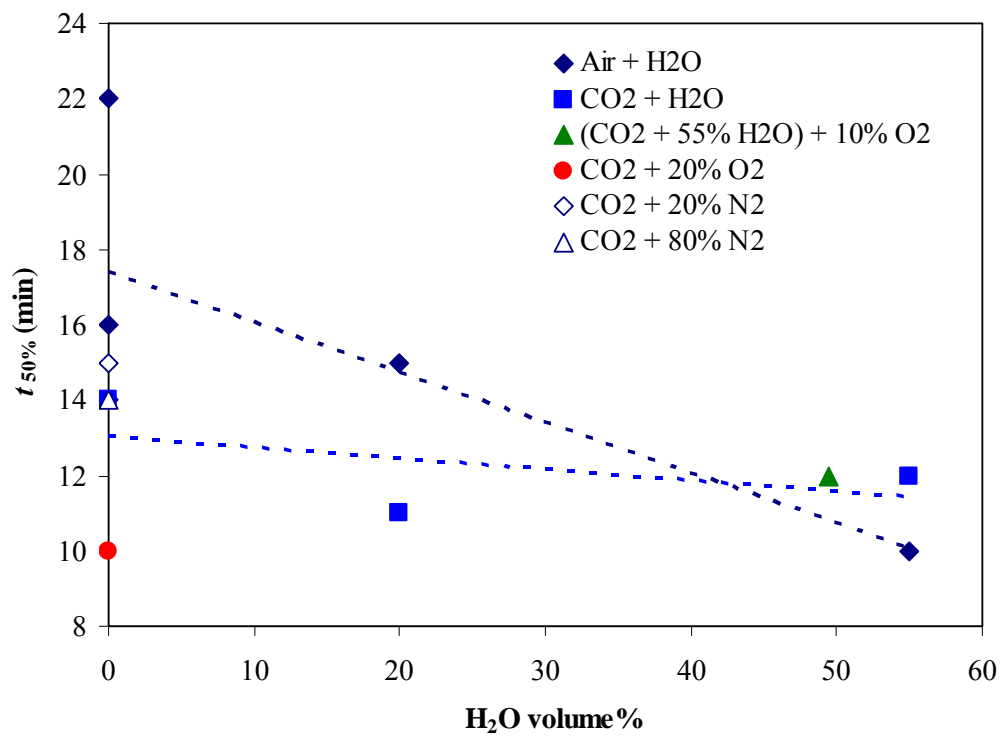
Figure 14. Foam Collapse Time to 50% of Maximum ψ versus H₂O Content

16
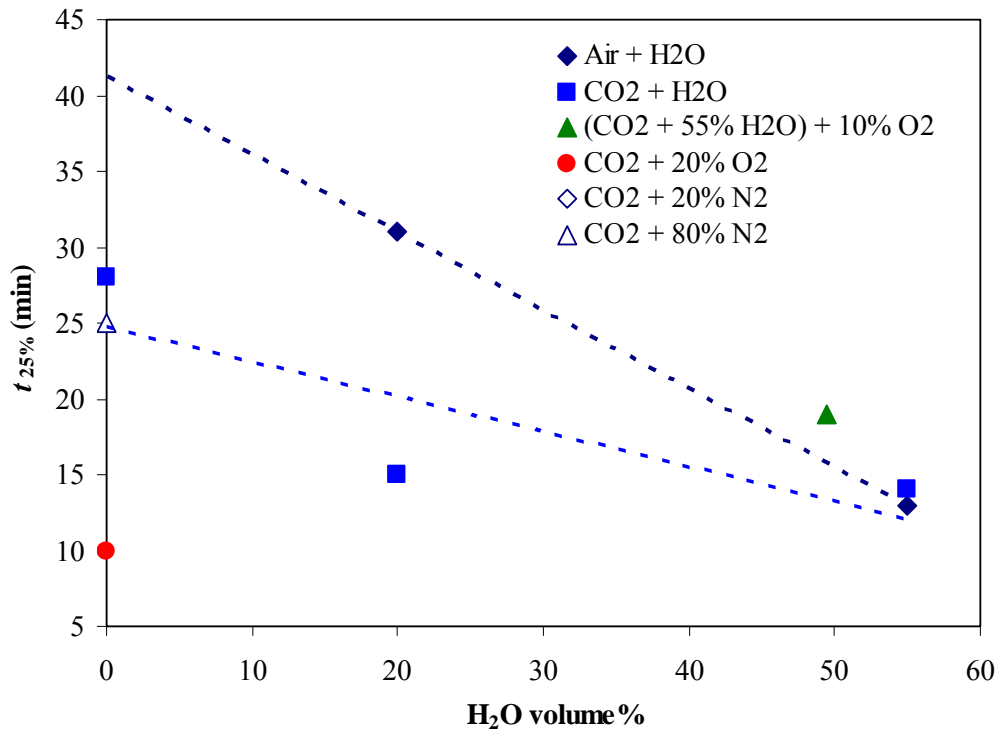
Figure 15. Foam Collapse Time to 25% of Maximum ψ versus H_2O Content

3.3 Discussion

3.3.1 Foam stability

Foam stability can be measured using $d\psi/dT$, ψ_{max}, or $t_{0.5}$. By all these measures, foam stability in E glass decreases with increasing humidity, most likely by the decreased viscosity of the melt film. Therefore, enhanced foaming observed in oxy-fired E-glass melting furnaces may not be explained by the effect of water on foam stability.

No noticeable effect of gas composition on foam stability (except for dry air), in particular no measurable effect of excess O_2 in simulated oxy-fired environment on the foam stability indicates that changing the furnace atmosphere, if such a change was technologically and economically feasible, is not expected to reduce the current level of foaming.

The foam-destabilizing effect of dry air as compared to other dry gases is not understood at present. However, additional experiments that would verify and elucidate this observation were not performed in the present study and their results do not appear relevant to the main objective of the current research, which is foam reduction in oxy-fired furnaces.

3.3.2 Effect of water on refining reactions

17

According to Laimböck (1998) and Beerkens et al. (1998), the increased foaming that occurs in oxy-fired furnaces is caused by the increased humidity of the furnace atmosphere. Water dissolves in glass and tends to establish the same partial pressure of H_2O in gas bubbles as in the atmosphere above the melt. As a result, the fining gases, such as SO_2 and O_2, are diluted in the bubbles. The decreased partial pressure of the fining gases in bubbles results in an increase of the driving force for the fining reactions. Thus, a substantially larger volume of gaseous phase is released per glass under humid atmosphere, leading to enhanced foaming. This dilution model is well developed mathematically and is supported by strong experimental evidence from foaming studies conducted on soda-lime glasses. The effect lower viscosity by increased humidity, mentioned above, seems insignificant for soda-lime glass, where the dilution effect dominates,

In our current experiments with E-glass except Test 13, the possibility of water dissolution in glass at early stages of melting and thus the dilution effect was minimized by introducing humid gas only after the batch reactions were completed. The Test 13 in which the humid gas (45% CO_2 + 55% H_2O) was introduced at early stages of melting did not produce any foam whereas Test 8 with same humid atmosphere introduced at 1250°C produced foam. The reason for the lack of foaming in Test 13 is most likely an early loss of sulfate due to higher water content at early stages of melting, as discussed below.

Sulfate loss due to evaporation proceeds at temperatures well below sulfate begins to decompose. Sulfate evaporation is promoted by humidity. If losses due to evaporation are such that the partial pressures of SO_2 and O_2 in glass are too low to cause an appreciable growth of bubbles, no foaming will occur. This may be a possible explanation for the absence of foam in Test 13. The proof of this hypothesis can be obtained if the glass is analyzed for the content of SO_3 for the samples taken at several stages of melting. This was unfortunately beyond the scope of the present work.

Laimböck measured the sulfate loss in soda lime glass at early stages of melting as well as during fining. The initial SO_3 concentration was 0.66 mass%. The SO_3 concentration before fining was 0.55~0.53 mass% and 0.32~0.15 mass% after fining. These numbers are large compared to the as-batched SO_3 concentration in E-glass of the present study, which was 0.17 mass%; roughly a half of this amount came from Na_2SO_4 and the rest was impurity from other raw materials (mainly colemanite). Estimating that SO_3 concentration dropped to 0.01 mass% after fining (typical measured concentration in the product glass), and considering possible evaporation of sulfate before fining, the loss of SO_3 during foaming was less than 0.16 mass%. Hence, only a small amount of sulfate is available for gas generation in the E glass as compared to soda-lime glass. Consequently, relatively small losses of sulfate from E-glass may be sufficient to decrease the gas generation rate beyond the critical level needed for foaming.

The lack of foaming in the pre-melted glass described in Section 2.4 can also be attributed to the loss of sulfate during the pre-melting by decomposition reaction and evaporation. The amount of sulfate decomposed during 2-h melting at 1380°C under ambient atmosphere was enough to prevent foaming and even reboil when heated at a temperature as high as 1500°C. This contrasts with the behavior of soda-lime glass refined at 1480°C that would reboil on heating as soon as the temperature exceeds 1480°C (used in Laimböck tests).

Accordingly, fining and foaming behaviors of E-glass and soda-lime glass in laboratory crucible test conditions are substantially different. However, the crucible test results may not be directly applicable to plant condition because the critical level of gas generation for foaming in plant will be different, primarily

because of the difference in size and geometry of the melt pool, which produces different thermal history of glass batch. For example, the as-melted materials below the batch pile in the glass furnace is remixed to the already refined melt so that the part of the gases generated by early decomposition of sulfate may also contribute to foaming. The observation that oxy-firing tends to increase the foam in E-glass suggests that the dilution effect on refining and foaming should also be applicable to E-glass melting in the commercial melting furnaces.

In a very simplistic argument, if the sulfate added to the batch is controlled solely by the refining behavior, like in a typical clear soda-lime glass, the dilution effect in oxy-fired condition would require smaller addition of sulfate to achieve the same refining efficiency and would result in the same foaming extent. However, when the sulfate in E-glass serves other purposes, such as redox control, in addition to refining, the sulfate addition may not be decreased to a sufficiently low level, which will result in increased foaming. This may explain why the oxy-fired E-glass furnaces produce more foam than air-fired.

3.3.3 Rate of Heating

The preliminary experiments were performed at two rates of heating, i.e., $\Phi = 5$ K/min and $\Phi = 10$ K/min. Figure 16 reproduces the linear portions of Figure 4. The dh/dT values for the foaming interval are 0.711 mm/K for the heating rate of 10 K/min and 0.299 mm/K for the heating rate of 5 K/min. Table 3 displays the $d\psi/dT$ and $d\psi/dt$ values for the two heating rates, showing that $d\psi/dT$ increases nearly linearly with Φ, thus $d\psi/dt$ is proportional to Φ^2. Based on the two data points available,

$$d\psi/dt = \chi \Phi^2 \qquad (4)$$

where $\chi = 0.738$ s/K^2.

Equation (4) implies that the higher throughput of the furnace would increase foaming because it would lead to a higher Φ ($= dT/dt = vdT/ds$), where v is the melt velocity and s is the distance along the melt trajectory. With an increased throughput, v is likely to increase in the fining zone of the furnace.

19
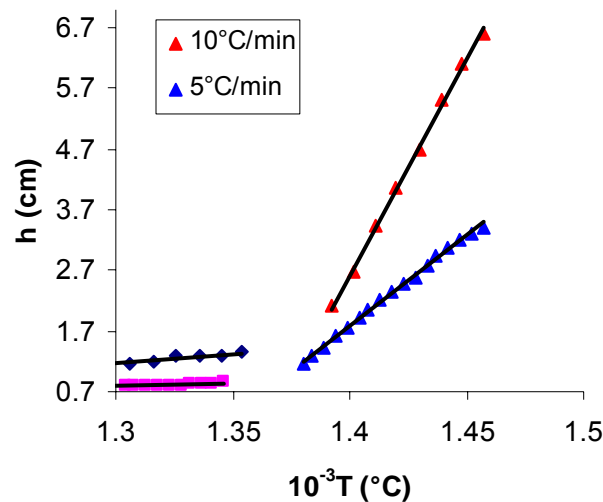
Figure 16. Sample Height versus Temperature, Open Air Experiment

Table 3. dψ/dT and dψ/dt from Open Air Experiment

dT/dt (°C/min)	m_B (g)	dh/dT (mm/°C)	dψ/dT (°C^{-1})	dψ/dt (s^{-1})
5	4	0.299	0.064	0.0053
10	5	0.711	0.122	0.0203

It seems premature to draw conclusions from just two preliminary data points. However, if these data points indicate a technologically important result, it is of interest to see if there is any scientific basis for such a phenomenon. The gas-phase balance law can be stated as

$$\dot{\psi} = \dot{\psi}_{ev} - \dot{\psi}_{rel} \tag{5}$$

where the dot above the symbol stands for the time derivative and the subscripts *ev* and *rel* stand for gas evolved and gas released. The rate of gas evolution into bubbles is proportional to the difference of the partial pressures of the fining gas in the melt and in a bubble (Δp), the bubble surface area per melt volume (a_B), and the diffusion coefficient of the fining gas in the melt. Since the diffusion coefficient is roughly proportional to melt viscosity (η), we can write

$$\dot{\psi}_{ev} = k_{ev} \frac{\Delta p a_B}{\eta} \tag{6}$$

where k_{ev} is a constant. The rate of gas release is directly proportional to the melt top surface area (a_G) and indirectly to the melt viscosity, the dominant property for foam stability. Thus,

$$\dot{\psi}_{rel} = k_{rel} \frac{a_G}{\eta} \tag{7}$$

where k_{ev} is a constant.

In Equations (6) and (7), none of the parameters Δp, η, and a_G depends on Φ. The only parameter that can depend on Φ is a_B. Connecting Equation (4) to (7) and expressing a_B, we obtain

$$a_B = \frac{\chi \eta \Phi^2 + k_{rel} a_G}{k_{ev} \Delta p} \tag{8}$$

Equation (8) can be simplified to

$$a_B = a_0 + \left(\frac{\Phi}{\Phi_0}\right)^2 \qquad (9)$$

where a_0 and Φ_0 are coefficients defined by Equations (8) and (9). Thus, the foam increase rate is proportional to Φ^2 because the bubble surface are per melt volume is proportional to Φ^2. To elucidate this connection, let us consider two extreme cases: extremely slow heating, i.e., $\Phi \to 0$, and extremely fast heating, i.e., $\Phi \to \infty$.

If the heating of melt is very slow ($\Phi \to 0$), Equation (9) reduces to $a_B = a_0$. Hence, the bubble area is constant. This represents a steady state between gas evolution and gas release, i.e., $d\psi/dt = 0$. The foam extent is low and remains constant until all bubbles are released.

If the heating of melt is very fast ($\Phi \to \infty$), Equation (9) reduces to $a_B = (\Phi/\Phi_0)^2$. Hence, temperature increases rapidly, bubbles grow fast and the bubble surface are in the melt is proportional to Φ^2. This represents a no-release state. A more detailed analysis would show that not only the bubble surface area is large, but also the melt is stretched into thin films, from which the gas release is fast because of short distances for diffusion. Therefore, the melt height increases rapidly to the point at which all excess fining gas is released into the bubbles. At this point, the foam rapidly collapses unless it gets stabilized.

To summarize, the strong effect of the rate of heating on foaming is possible, though the quantitative experimental data for it is sparse. The above analysis also signifies that the thermal history of glass can play an important role in determining the extent of foaming.

4.0   Conclusions and Recommendations

The results of foaming experiments with varying gas atmospheres conducted in this study point that the higher foaming in oxy-fired furnace (compared to air-fired) in E-glass production is not caused by the effect of water on foam stability, which contradicts the general hypothesis. The higher foaming in oxy-fired E-glass furnace can be attributed to the dilution effect of water on sulfate decomposition, discussed in the literature primarily for the soda-lime glasses. However, the difference is that the sulfate in E-glass has other function in addition to refining, which may prevent the decrease of sulfate to a sufficiently low level to compensate the increased refining gas generation in oxy-fired furnaces.

The possibility that small change of gas atmosphere may have a significant effect on foam stability was not confirmed at least within the atmospheres with varying fraction of N_2, CO_2, and O_2 tested in this study. The strong effect of heating rate on foaming was mathematically formulated, which agrees with the industry experience of higher foaming at higher throughput. It may be possible to find the furnace operation conditions that lead to optimal overall melt trajectory for minimum foaming using furnace modeling tools.

Two possible approaches to decrease the foam in oxy-fired furnace can considered:

1.   Use of furnace modeling tools to optimize the furnace operation conditions for minimum foam generations

2.   Use of certain external means to destabilize the foam, for example, by localized heating using microwave, laser, or IR heating or by localized disturbance using ultrasound waves.

The specific methods need to be identified from more detailed experimental studies. The first recommended step is to perform additional tests on foam generation to confirm above conclusions because they are based on very limited tests with E-glass:
- Analyze the sulfate retention at different stages of melting
- Study the effect of gas compositions inside and outside of bubbles using steady-state foams
- Study the effect of changing gas compositions using transient and/or steady-state foams

The next step would be to identify specific methods to reduce the foam based on either approach discussed above:

1.   Development of furnace modeling tools
- Develop a foam sub-model to predict the foaming extent or formulate foaming indices that can be calculated from glass flow model results
- Generate quantitative data needed for the development of foam sub-model and/or foaming indices formulation, such as the effect of thermal history and batch thickness (height) on foam generation and the effect of temperature, lamellar thickness, and other factors on foam film breakage.

2.   Foam destabilization studies
- Perform feasibility or literature studies to select the candidate method for further study

- Develop experimental methods to test foam stability by applying external means to transient or steady-state foams generated in the crucible melts
- Conduct lab tests to confirm the suggested method and identify the variables that control the foam destabilization
- Perform scale-up tests or engineering studies, if necessary, before plant application

5.0   References

Beerkens, R., P. Laimbök, and S. Kobayashi. 1998. "The Effect of Water on Fining, Foaming and Redox of Sulfate Containing Glass Malts," in Advances in Fusion and Processing of Glass II (Edited by A. G. Clare and L. E. Jones), Ceramic Transactions, Vol. 82, 43-49.

Cable M. and C. G. Rasul and J. Savage. 1968. "Laboratory investigation of foaming and reboil in soda-lime-silicate melts," Glass Technology, Vol. 9, No.2, 25-31.

Cooper, C. F. and Kitchener. 1959. "The foaming of molten silicates," Journal of the Iron and Steel Institute, pp.48-55.

Hrma, P. 1982. "Thermodynamics of Batch Melting," *Glastech. Ber*. 55 [7] 138-150.

Hrma, P. and D. Kim. 1994. "Sulfate Mass Balance and Foaming Threshold in a Soda-Lime Glass," *Glass Technol.*, 35 [3] 128-34.

Kappel, J, R. Conradt, and H. Scholze. 1987. "Foaming Behavior on Glass Melts," Glastech. Ber., Vol. 60, No.6, 189-201.

Kim, D. and P. Hrma. 1991. "Foaming in Glass Melts Produced by Sodium Sulfate Decomposition under Isothermal Conditions," *J. Am. Ceram. Soc.*, 74 [3] 551-55.

Kim, D. and P. Hrma. 1992. "Foaming in Glass Melts Produced by Sodium Sulfate Decomposition under Ramp Heating Conditions," *J. Am. Ceram. Soc.*, 75 [11] 2959-63.

Laimböck, P. R. 1998. "Foaming of glass melts," University of Technology, Eindhoven, Ph.D. Thesis.

Parikh, N. M. 1958. "Effect of atmosphere on surface tension of glass," Journal of the American Ceramic Society, Vol. 41, pp. 18-228.

Pilon, L. and R. Viskanta. 2003. "Minimum superficial gas velocity for onset of foaming," Chemical Engineering and Processing, Vol. 43, 149-160.

Zhang Y. and R.J. Fruehan. 1995. "Effect of the Bubble Size and Chemical Reactions on Slag Foaming," Metallurgical and Materials Transaction B, 26B 803-812.